Schlumberger

1985年中国测井评价会议

WELL EVALUATION CONFERENCE CHINA 1985

The preparation of this document was co-ordinated by J.S. Mok with the collaboration of:

D.J. Alardo, A. Cerny, S. des Ligneris, O. Faivre, J.E. Johansson, C.S. Kabir, Y.G. Maria-Sube, G.G. Shanor, A.M. Sibbit,

and contributions from:

G. Beylkin, J. Buss, M.E. Josso, C.C. Laughlin, Li Gansheng, Lin Zubin, D. Miller, M. Oristaglio, R.A. Plumb, Wang Shenyang, Wu Minde, Zha Quanheng, Zhai Guanming.

9.液相持留量
10.滑脱速度
11.气体对比速度
12.气体流速
13.液体流速
14.原油密度
15.气体密度

图 9.4-14a 到 9.4-14d 是选出的一组图，表示上述变量与输入的实测压力数据的关系，还有三张图表示 Glaso 物理特性与井内测得的压力的关系。

DIFLOW 程序可以解释出在 1 层底部的下边有流体流入井内。当有了涡轮流量计数据和压差密度计数据时，还可以解释双相流动。用 TUPPRA 确定出一些最佳相关式，如 Glaso 的物理特性相关式，Aziz 和 Govier 的压力降相关式，使我们能够选用最合适的一组相关式。因此能够校正 DIFLOW 中所用的流体特性，确定流体进入井内的位置。

试验室对油层流体样品的分析取到了油气性质的数据，在这种情况下，TUPPRA 就可以使用这些特性数据，不用一般的相关式。

12. gas flowrate
13. liquid flowrate
14. oil density
15. gas density

Figs. 9.4–14a to 9.4–14d show a selection of some of the plots listed above against input measured pressure data.

Below the bottom of Zone 1, fluid entry into the wellbore can be interpreted using the DIFLOW program to make a diphasic flow interpretation when both spinner and gradiomanometer data are available. The determination of the best correlations by TUPPRA such as the physical properties of Glaso, and pressure drop correlation of Aziz and Govier allow us to use the most appropriate pair of correlations; thus, correct fluid properties in DIFLOW could be used to solve for the fluid entry.

For those cases where the oil and gas properties are known from laboratory analysis of reservoir fluid samples, these properties may be used in TUPPRA instead of general correlations.

References

1. Leach, B.C., Jameson, J.B., Smolen, J.J., and Nicolas Y.: "The Full Bore Flowmeter", paper SPE 5089 presented at the 49th Annual Fall Meeting, Houston, Tx., Oct. 6–9, 1974.
2. *Production Log Interpretation Charts*, Schlumberger 1973.

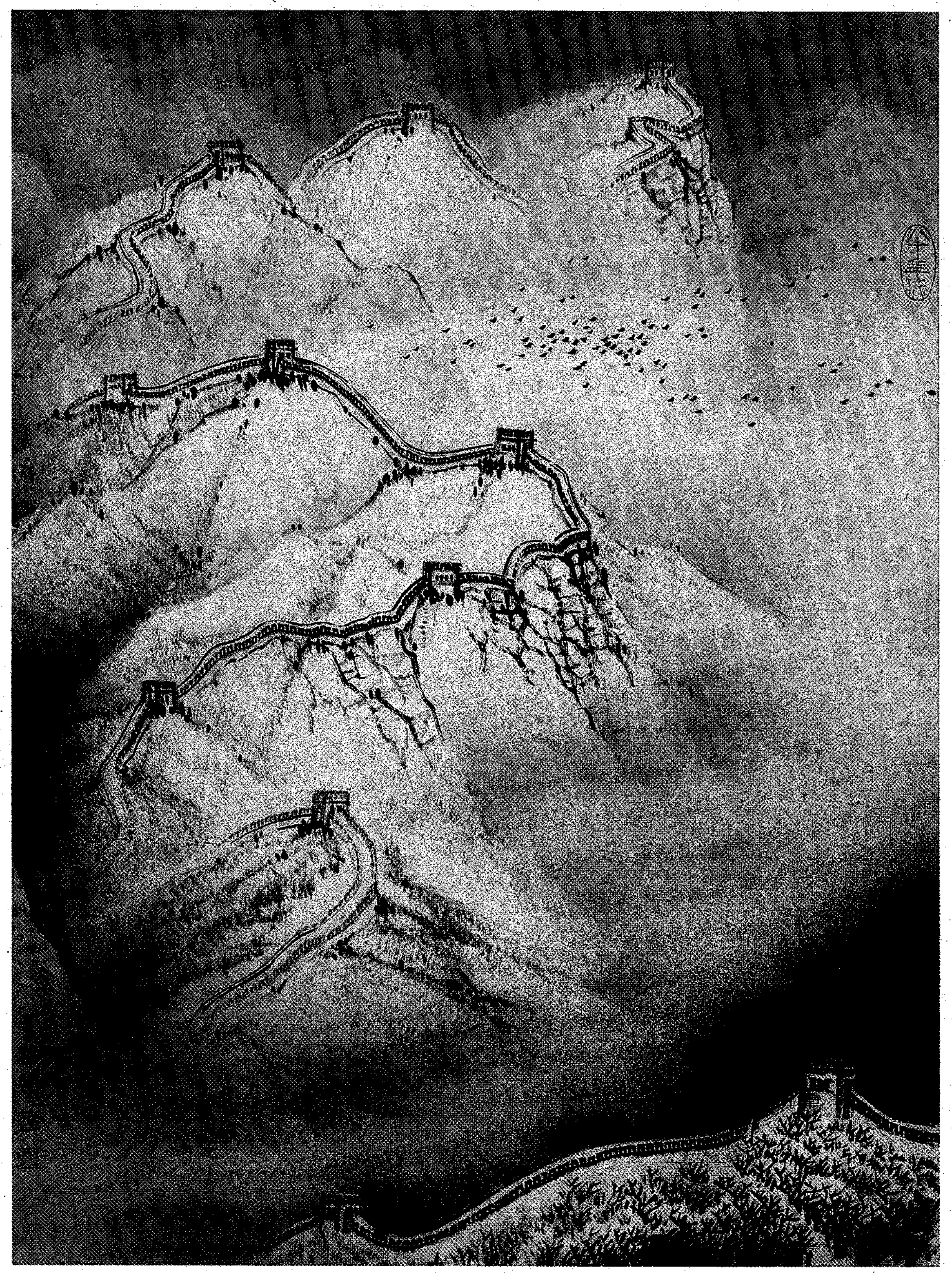

10

测井研究的几个论题

SELECTED TOPICS IN WIRELINE RESEARCH

10.1 关于地震偏移校正的新见解

D. Miller, M. Oristaglio, and G. Beylkin
斯伦贝谢·道尔研究中心

10.1 A NEW SLANT ON SEISMIC MIGRATION

D. Miller, M. Oristaglio, and G. Beylkin
Schlumberger — Doll Research, Ridgefield

地震偏移校正的一项新方法使早期的几何作图法诸如绕射和波前叠加以及与此有关的线性速度反演和广义雷佟变换 (GRT) 更趋成熟。该方法把偏移校正再次看作为层析 x 射线摄影法的一种形式，其中包括重新构成一个函数（速度变动）的问题，此函数是由其本身在面簇（等时面）上的积分所构成。这项理论是建立在用几何光学和 GRT 的反演求解波动方程式的基础上。该方法能够处理在震源和检波器任意排列时速度的纵向和横向变化。此外，在特定的背景速度恒定及零偏置的地震试验情况下，可得到其反演运算，类似于标准的基尔荷夫偏移校正。地面地震和 VSP（垂直地震剖面）试验组合的模拟试验说明在震源和检波器不同排列时该方法的分辨率。

引言

目前井下地震数据的分类按其数量级可由全波波形声测井(厘米到米数量级)到多级偏置的 VSP（垂直地震剖面）（米到公里数量级），且在量与复杂性方面均可与地面地震数据相匹敌。对地震数据处理这一问题只不过是使用同一方法去处理整个范围的地面和井下地震数据。其中获取最终地震成果的重要方法之一是得到地下构造图，该过程通常称为偏移校正。

一般的概念，偏移校正是指由地震反射波也就是说由地面记录的地震反射波所构制的地层速度图（参看 Robinson 的书，1983 或 Gazdag 和 Sguazzero, 1984的评论文章）。最早的偏移校正法基于简单的几何概念 (Hagedoorn, 1954)，但到70年代，这些方法已被废弃，并由基于波动方程的新方法所取代 (Claerbout, 1976)。正如 Gazdag 和 Sguazzero (1984) 在评论中指出的那样：“尽管这些（几何）偏移校正方法作出了很好的论断，既直观又明确，但这些方法本身往往并未完全根据声学原理。”

然而，对偏置 VSP 的偏移校正所发展的方法中，现在我们找到了一种新的地震偏移校正法，该方法不仅使早期的几何方法更趋完善，而且也更适合于处理复杂地质构造及震源和检波器异常排列的情况 (Miller, Oristaglio 和 Beylkin, 1984)。甚至，后两点

A new approach to seismic migration formalizes the early geometric methods such as the diffraction and wavefront stacks by relating them to linearized velocity inversion and the Generalized Radon Transform (GRT). This approach recasts migration as a form of tomography in which the problem is to reconstruct a function (velocity perturbation) from its integrals over a family of surfaces (isochrons). The theory rests on a solution of the wave equation by geometrical optics and an inversion formula for the GRT. This method can handle both lateral and vertical variations in velocity as well as arbitrary configurations of sources and receivers. Moreover, when specialized to constant background velocity and zero-offset seismic experiments, it yields an inversion algorithm that resembles standard Kirchhoff migration. Synthetic examples of a combined surface seismic and VSP experiment illustrate the resolution of the method for different combinations of sources and receivers.

Introduction

Borehole seismic data now range in scale from the full-waveform sonic log (cm to m scale) to the multi-offset VSP (m to km scale) and have begun to rival surface seismic data in their volume and complexity. A challenge for seismic data processing is simply to treat the full range of seismic data, surface and borehole, in a unified way. One important way in which seismic data are finalized is in pictures of subsurface structures, a process that is commonly called migration.

Traditionally, migration has meant constructing an image of the earth from seismic reflections — in fact, from seismic reflections recorded at the earth's surface (Robinson, 1983; Gazdag and Sguazzero, 1984). The earliest migration methods were based on simple geometrical ideas (Hagedoorn, 1954). In the 1970's, however, these methods were largely abandoned in favor of methods based on the wave equation (Claerbout, 1976). As Gazdag and Sguazzero (1984) point out in their review, "while these (geometrical) migration procedures make good sense and are intuitively obvious, they are not based on a completely sound theory".

Recently, however, in developing ways to migrate offset VSPs, we have found a new approach to seismic migration which not only formalizes the early geometrical methods, but is also flexible enough to handle both complex structures and unusual configurations of sources and receivers (Miller, Oristaglio, and Beylkin, 1984). Moreover, these latter two features needed to migrate most kinds of borehole seismic data, are difficult to obtain with the popular methods used for surface seismic migration.

The underlying idea of the new approach is very simple: That seismic migration can be viewed as the inverse problem of reconstructing a function — in this case, the earth's velocity structure — from its integrals over a family of surfaces. This reconstruction problem has arisen independently in many scientific fields, with the most dramatic results coming from the field of medical imaging (e.g. x-ray tomography). And, although our methods and their application to seismic data are new,

对大多数的井下地震数据偏移校正是很需要的，而要用地面地震偏移校正传统的方法来达到这一目的是困难的。

这一新方法的基本概念是很简单的：地震偏移校正可看作是构成一个新函数（本文中的地层地震波速度结构）的反演问题，该函数是由其本身在面簇上的积分构成的。这种重构新函数的问题在许多科学领域已独立出现，在医学摄象领域有了最显著的成果（如x-射线摄影法）。虽然，我们的方法及其对地震数据处理的应用是新的，但这些方法的数字基础可追溯至早期1900年代雷佟的著作(Deans, 1983)。

由雷佟提出并解决的问题是重构一个二维新函数的问题，该函数由其本身在直线上的积分所构成，通常称为"投影"。雷佟的方法形成了著名的经典雷佟变换的基础。由函数本身在任意面簇上的积分重构这一函数的问题涉及广义雷佟变换。在此，我们把地震偏移校正的理论概括为广义雷佟变换，且用模拟试验给出对这些问题的求解。由这些示例表明该方法比用地震数据通常的处理方法所具有的一些优点。

几何偏移校正

偏移校正的基本原理是：地层上的每一点都可采用测定该点散射场的方法经作图作出。这一原理最直接的应用是经典绕射叠加，它后来发展为波论的吉尔荷夫偏移校正 (French, 1975)。绕射叠加是一种沿最大凸状哈格杜恩 (1954) 地震记录曲线的求和，也就是所谓的绕射曲线或时距曲面。对于一个固定的震源点 $\underline{s}$ 和图象点 $\underline{x}$，时距曲面 R 是检波器 $\underline{r}$ 和时间 t 的轨迹，t 是由图象点能量能够到达检波器的时间。严格地说，时距曲面可由$(\underline{r},t)$组对来描述，即对每个检波器 $\underline{r}$，它的时间 t 将是震源——图象点和图象点——检波器之间总的历行时间，即

$$R_{\underline{x}} = [(\underline{r},t): t = \tau(\underline{r},\underline{x}) + \tau(\underline{x},\underline{s})] \quad \ldots\ldots \quad (1)$$

式中，$\tau(\underline{x},\underline{y})$是点$\underline{x}$和$\underline{y}$之间的历行时间。

绕射叠加的启示性解释如下：对一个给定的点 $\underline{x}$，我们沿着由该点散射能量对应的时距曲面进行数值积分检查在该点是存在反射层。如果点 $\underline{x}$ 存在反射层，其相应的能量将沿曲线散布并有大的输出。另

their mathematical basis dates back to the work of Radon in the early 1900's (Deans, 1983).

The problem posed and solved by Radon was that of reconstructing a two-dimensional function from its integrals over straight lines, often called "projections". Radon's methods from the basis of what is now known as the classical Radon Transform. The problem of reconstructing a function from its integrals over arbitrary surfaces involves the Generalized Radon Transform. Here, we briefly review the theory that recasts seismic migration as a problem of the Generalized Radon Transform, and we illustrate our solution to this problem with synthetic examples. These examples also show some of the advantages to be gained by a unified treatment of seismic data.

Geometrical Migration

A basic principle of migration is that each point in the earth can be imaged by detecting the field scattered by that point. The most direct use of this principle was the classical diffraction stack, which later evolved into wave-theoretical Kirchhoff migration (French, 1975). The diffraction stack is a summation of the seismograms along Hagedoorn's (1954) curve of maximum convexity, also known as a diffraction curve or reflection-time surface. For a fixed source position $\underline{s}$ and image point $\underline{x}$, the reflection-time surface R is the locus of receiver positions $\underline{r}$ and times t at which energy from the image point could arrive. Mathematically, the reflection-time surface can be described as the set of $(\underline{r},t)$ pairs, such that for each receiver $\underline{r}$, the time t corresponds to the total traveltime between source, image point, and receiver; that is,

$$R_{\underline{x}} = [(\underline{r},t): t = \tau(\underline{r},\underline{x}) + \tau(\underline{x},\underline{s})] \quad \ldots\ldots \quad (1)$$

where $\tau(\underline{x},\underline{y})$ is the traveltime between points $\underline{x}$ and $\underline{y}$.

The heuristic interpretation of the diffraction stack is as follows: for a given point $\underline{x}$, we check if there is a reflector at that point by integrating the data along the time-distance curve corresponding to energy scattered from the point. If a reflector is present at the point $\underline{x}$, then coherent energy should be distributed along the curve and will sum to a large output. Random noise, on the other hand, will cancel. Repeating the diffraction stack for all image points should thus highlight coherent reflectors.

Dual to the reflection-time surface R is the isochron surface I, defined by fixing a point $(\underline{r},t)$ in the data and finding the locus of image points $\underline{x}$ that could contribute energy to the field observed at the chosen data point. Mathematically, we have for the isochron surface,

$$I_{\underline{r},t} = [\underline{x}: t = \tau(\underline{r},\underline{x}) + \tau(\underline{x},\underline{s})] \quad \ldots\ldots \quad (2)$$

where in this case, given $\underline{r}$ and t (and fixed $\underline{s}$), we obtain a locus of image points that satisfy a traveltime constraint.

The geometrical idea embodied in equations 1 and 2 is that the traveltime τ induces a natural correspondence

一方面，随机噪声将消失。对全部图象点进行重复绕射叠加，这些反射层将更显突出、清晰。

两倍的时距曲面 R，即是等时面 I，该等时面 I 是用固定数据点$(\underline{r},t)$并搜寻图象点 $\underline{x}$ 的轨迹的方法来确定的，在所选择的数据点上能够观测到 $\underline{x}$ 散布能量所及的场。严格地说，对等时面有，

$$I_{\underline{r},t} = [\underline{x}: t = \tau(\underline{r},\underline{x}) + \tau(\underline{x},\underline{s})] \quad \ldots\ldots \quad (2)$$

在该情况下，当给定 $\underline{r}$ 和 t（并固定 $\underline{s}$），我们得到图象点的轨迹，并满足所约定的历行时间。

方程1和2的几何概念是：历行时间 τ 使得一个空间中（数据或图象）的点和另一空间中的面之间一一自然对应。此外，众所周知，使用绕射叠加的偏移校正与覆盖长度或在每个数据点$(\underline{r},t)$沿它相应的等时面 $I_{\underline{r},t}$ 所记录振幅的反向投影（公切面或波前叠加）是等效的。

广义雷佟变换

在广义雷佟变换(GRT)的理论中自然也出现前述的几何作图。对于三维函数 $f(\underline{x})$，其经典雷佟变换（在地球物理文献中经常称为斜面叠加）为

$$\hat{f}(\underline{\xi},p) = \int d^3\underline{x}\,\delta(p - \underline{\xi}\cdot\underline{x})\,f(\underline{x}) \quad \ldots\ldots \quad (3)$$

式中$\hat{f}(\underline{\xi},p)$是 $f(\underline{x})$的雷佟变换，$\underline{\xi}$ 是单位矢量，p 为变换参数。经典雷佟变换表达了点函数$f(\underline{x})$与在 $p = \underline{\xi}\cdot\underline{x}$ 面簇上 $f(\underline{x})$的积分的关系，面 $p = \underline{\xi}\cdot\underline{x}$ 是用旋转垂直于面 $\underline{\xi}$ 的单位矢量和，改变参数 p 以确定该面（$\underline{\xi}\cdot\underline{x}$）至原点的距离的方法来确定的。在更为广义的面上，其加权函数的积分表示广义雷佟变换。

结合具有GRT的偏移校正，我们认为标量波动方程线性速度的反演问题是

$$\nabla^2 u(\underline{x},\omega) + \frac{\omega^2}{c^2(\underline{x})} u(\underline{x},\omega) = -\delta(\underline{x} - \underline{s}) \quad \ldots\ldots \quad (4)$$

式中 $u(\underline{x},\omega)$ 是总声压场，$\underline{s}$ 为震源点，ω 为频率，及$c(\underline{x})$为可变的声波速度。设

$$c^{-2}(\underline{x}) = c_o^{-2}(\underline{x}) + f(\underline{x}),$$

between points in one space (data or image) and surfaces in the other. Moreover, it is well-known that migration by diffraction stack is equivalent to smearing or backprojecting the recorded amplitude at each data point $(\underline{r},t)$ along its corresponding isochron surface $I_{\underline{r},t}$ (common-tangent or wavefront stack).

The Generalized Radon Transform

The geometrical constructions described above also arise naturally in the theory of the Generalized Radon Transform (GRT). First recall the classical Radon Transform (often called a slant stack in the geophysics literature) for a three-dimensional function $f(\underline{x})$,

$$\hat{f}(\underline{\xi},p) = \int d^3\underline{x}\,\delta(p - \underline{\xi}\cdot\underline{x})\,f(\underline{x}) \quad \ldots\ldots \quad (3)$$

Here, $\hat{f}(\underline{\xi},p)$ is the Radon Transform of $f(\underline{x})$, $\underline{\xi}$ is a unit vector, and p is a transform parameter. The classical Radon Transform relates a point function $f(\underline{x})$ to its integrals over the family of planes $p = \underline{\xi}\cdot\underline{x}$ obtained by rotating the unit vector normal to the plane $\underline{\xi}$ and varying the parameter p that determines the distance of the plane from the origin. Integrals with a weight function over more general surfaces represent the Generalized Radon Transform.

To connect migration with GRT, we consider the linearized velocity inversion problem for the scalar wave equation,

$$\nabla^2 u(\underline{x},\omega) + \frac{\omega^2}{c^2(\underline{x})} u(\underline{x},\omega) = -\delta(\underline{x} - \underline{s}) \quad \ldots\ldots \quad (4)$$

where $u(\underline{x},\omega)$ is the total acoustic pressure field, $\underline{s}$ is the source position, ω is the frequency, and $c(\underline{x})$ is the variable acoustic velocity. Letting

$$c^{-2}(\underline{x}) = c_o^{-2}(\underline{x}) + f(\underline{x}),$$

where $c_o(\underline{x})$ is a known reference velocity (not necessarily constant) and $f(\underline{x})$ is the velocity perturbation to be determined, we obtain by standard techniques the following linearized integral equation for f

$$u_{sc}(\underline{r},\omega) = \omega^2 \int d^3\underline{x}\, G_o(\underline{r},\underline{x},\omega)\, G_o(\underline{x},\underline{s},\omega) f(\underline{x}) \quad \ldots\ldots \quad (5)$$

Here, $G_o(\underline{x},\underline{y},\omega)$ is the Green function for the reference medium $c_o(\underline{x})$ and $u_{sc}(\underline{r},\omega) \equiv u - G_o$ is the scattered acoustic wavefield recorded at the receiver position $\underline{r}$.

We now set $G_o(\underline{x},\underline{y},\omega) = A(\underline{x},\underline{y}) \exp[i\omega\tau(\underline{x},\underline{y})]$ and use the geometrical optics approximation for the amplitude A and phase $\omega\tau$ of the Green function. Substituting for G_o in Eq. 5 and inverse Fourier transforming to the time-domain gives

$$u_{sc}(\underline{r},t) = -\frac{\partial^2}{\partial t^2}\int d^3\underline{x}\, A(\underline{r},\underline{x})\, A(\underline{x},\underline{s})\, \delta[t - \tau(\underline{r},\underline{x}) - \tau(\underline{x},\underline{s})] f(\underline{x}) \quad \ldots\ldots \quad (6)$$

Since $\tau(\underline{x},\underline{y})$ is the traveltime between $\underline{x}$ and $\underline{y}$, this equation relates the scattered acoustic pressure recorded at $(\underline{r},t)$ to a weighted integral of the unknown function $f(\underline{x})$ over the isochron surface $I_{\underline{r},t}$ (Eq. 2). For example, when the reference velocity c_o is constant, the amplitude term A is just $1/4\pi|\underline{x} - \underline{y}|$, where $|\underline{x} - \underline{y}|$ is the distance between $\underline{x}$ and $\underline{y}$, $\tau = |\underline{x} - \underline{y}|/c_o$ is the straight-line traveltime, and the isochron surface is an ellipsoid.

式中 $c_o(\underline{x})$ 是已知参考速度（未必为常数）及 $f(\underline{x})$ 是需确定的速度变动，使用标准技术我们得到 f 的下列线性积分方程，

$$u_{sc}(\underline{r},\omega) = \omega^2 \int d^3\underline{x}\, G_o(\underline{r},\underline{x},\omega)\, G_o(\underline{x},\underline{s},\omega) f(\underline{x}) \quad \ldots\ldots (5)$$

式中 $G_o(\underline{x},\underline{y},\omega)$ 是参考介质的参考速度 $c_o(\underline{x})$ 的格林函数，$u_{sc}(\underline{r},\omega) \equiv u - G_o$ 是在检波器 $\underline{r}$ 点记录的散射声法的波场。、

现在令 $G_o(\underline{x},\underline{y},\omega) = A(\underline{x},\underline{y})\exp[i\omega\tau(\underline{x},\underline{y})]$ 并对格林函数的振幅 A 和相位 $\omega\tau$ 可近似应用几何光学法。在方程 5 中代换 G_o 并进行时域的反富立 (Fourier) 变换给出

$$u_{sc}(\underline{r},t) = -\frac{\partial^2}{\partial t^2}\int d^3\underline{x} A(\underline{r},\underline{x})\, A(\underline{x},\underline{s})\, \delta[t - \tau(\underline{r},\underline{x}) - \tau(\underline{x},\underline{s})] f(\underline{x}) \quad \ldots\ldots (6)$$

因为 $\tau(\underline{x},\underline{y})$ 是 $\underline{x}$ 和 $\underline{y}$ 之间的历行时间，该方程表达了在点 $(\underline{r},t)$ 所记录的散射声波压力与未知函数 $f(\underline{x})$ 在等时面 $I_{\underline{r},t}$ 上加权积分的关系（方程 2）。例如，当参考速度 c_o 为常数时，则振幅 A 正好等于 $1/4\pi|\underline{x}-\underline{y}|$，$|\underline{x}-\underline{y}|$ 为 $\underline{x}$ 和 $\underline{y}$ 之间的距离，$\tau = |\underline{x}-\underline{y}|/c_o$ 是直达历行时间，等时面为椭圆面。

反演和偏移校正

方程 6 的积分定义了未知的速度变动 f 的广义雷佟变换，它具有变换参量检波器点 $\underline{r}$ 和时间 t。用 $f^+(\underline{r},t)$ 表示广义雷佟变换，我们得到散射场与 f 的滤波的 GRT 成比例，即

$$u_{sc}(\underline{r},t) = -\frac{\partial^2}{\partial t^2} f^+(\underline{r},t) \quad \ldots\ldots (7)$$

为还原速度函数，我们对方程 6 求反。经典雷佟变换的逆公式"滤波的反向投影"为

$$f(\underline{x}) = -\frac{1}{8\pi^2}\int d^2\underline{\xi}\, \frac{\partial^2}{\partial p^2} f^{\hat{}}(\underline{\xi},p)\Big|_{p=\underline{\xi}\cdot\underline{x}} \quad \ldots\ldots (8)$$

式中含有滤波变换 $\partial^2 f^{\hat{}}/\partial p^2$ 通过图象点 x 在整个面簇上的积分。（方程 8 中的积分是在 $|\underline{\xi}| = 1$) 单位球面上的积分。）对于方程 6 求反，该公式提出一个通过图象点 $\underline{x}$ 在全部等时面上的广义反向投影，或

$$< f(\underline{x}) > = \int_R W(\underline{r},\underline{x},\underline{s})\, u_{sc}(\underline{r},t)\Big|_{t=\tau(\underline{r},\underline{x})+\tau(\underline{x},\underline{s})} \quad \ldots\ldots (9)$$

Inversion and Migration

The integral in Eq. 6 defines a Generalized Radon Transform of the unknown velocity perturbation f, with the transform parametrized by receiver position $\underline{r}$ and time t. Denoting it by $f^+(\underline{r},t)$, we have that the scattered field is proportional to the filtered GRT of f; i.e.,

$$u_{sc}(\underline{r},t) = -\frac{\partial^2}{\partial t^2} f^+(\underline{r},t) \quad \ldots\ldots (7)$$

To recover the velocity function, we invert Eq. 6. Recall the inversion formula "filtered backprojection" of the classical Radon Transform,
Transform,

$$f(\underline{x}) = -\frac{1}{8\pi^2}\int d^2\underline{\xi}\, \frac{\partial^2}{\partial p^2} f^{\hat{}}(\underline{\xi},p)\Big|_{p=\underline{\xi}\cdot\underline{x}} \quad \ldots\ldots (8)$$

which involves an integral of the filtered transform $\partial^2 f^{\hat{}}/\partial p^2$ over all planes passing through the image point $\underline{x}$. (The integral in Eq. 8 is over the unit sphere $|\underline{\xi}| = 1$). This formula suggests for the inversion of Eq. 6 a generalized backprojection over all isochron surfaces passing through an image point $\underline{x}$, or

$$< f(\underline{x}) > = \int_R W(\underline{r},\underline{x},\underline{s})\, u_{sc}(\underline{r},t)\Big|_{t=\tau(\underline{r},\underline{x})+\tau(\underline{x},\underline{s})} \quad \ldots\ldots (9)$$

Here, $< f(\underline{x}) >$ is the estimated value of the velocity function at the image point and W is a weighting factor which includes the appropriate measure for the integral. Note that Eq. 9 is just a weighted diffraction stack of the data over the reflection-time surface $R_{\underline{x}}$.

The weighting function W that follows from the inversion of the GRT in Beylkin (1982) is given by

$$W = \pi^{-2} c_o^{-3}(\underline{x})\, A^{-1}(\underline{r},\underline{x})\, A^{-1}(\underline{x},\underline{s})\, \cos^3\alpha(\underline{r},\underline{s})\, d^2\underline{\xi}(\underline{r},\underline{s}) \quad \ldots\ldots (10)$$

Here $\alpha(\underline{r},\underline{s})$ is half the angle between the incident and scattered rays at the image point $\underline{x}$ and $d^2\underline{\xi}(\underline{r},\underline{s})$ is the solid angle measure on the unit sphere surrounding $\underline{x}$ (see Fig. 10.1–1). The essential part of W is the factor $\cos^3\alpha d^2\underline{\xi}$. As shown in Fig. 10.1–1, this factor can be obtained by identifying each isochron surface with its tangent plane at the image point and then changing variables in the classical Radon formula (8).

The inversion given by equations 9 and 10 is only a partial solution to the reconstruction problem; more precisely, it is the first term of a formal asymptotic solution of the integral Eq. 6 (Beylkin, 1982). Nevertheless, it can be shown that what is accurately recovered by this first term are the (locations of) discontinuities in the function f— that is, discontinuities in the velocity field. This is the interpretation normally given to migrated depth sections and, in part, it formalizes the intuitive notion of a seismic image.

For a general inhomogeneous reference velocity $c_o(\underline{x})$, the weight function W must be determined numerically by ray tracing. But for constant c_o and certain source-receiver geometries, W can be determined analytically. For example, with zero-offset surface experiments — i.e., with $\underline{s} = \underline{r} = (r_1,r_2,r_3 = 0)$ — and with constant background velocity, Eq. 9 becomes

式中 $< f(\underline{x}) >$ 是速度函数在图象点上的估计值；W 是一个包含与积分相应量级的加权因子。注意方程 9 正是在时距曲面 R_x 上数据的加权绕射叠加。

在 Beylkin (1982) 的文献中，继续对 GRT 进行反演运算，可给出加权函数 W，

$$W = \pi^{-2} c_o^{-3}(\underline{x})\, A^{-1}(\underline{r},\underline{x})\, A^{-1}(\underline{x},\underline{s})\, \cos^3\alpha(\underline{r},\underline{s})\, d^2\underline{\xi}(\underline{r},\underline{s}) \quad \ldots\ldots (10)$$

式中 $\alpha(\underline{r},\underline{s})$ 是在图象点 $\underline{x}$ 入射线和散射线间夹角之半，$d^2\underline{\xi}(\underline{r},\underline{s})$ 是 $\underline{x}$ 点周围单位球上的立体角（见图 10.1–1）。$\cos^3\alpha d^2\underline{\xi}$. 因子是 W 的主要部分。在图象点上鉴别每一等时面及其切面，其后在经典雷佟公式 8 中改变变量，可求出 $\cos^3\alpha d^2\underline{\xi}$ 因子。

由式 9 和式 10 给出的反运算公式只是重构问题的特解，更精确些说，它是积分方程 6 形式渐近解的第一项 (Beylkin, 1982)。可以看出，由第一项所精确复现的正是在函数 f 不连续的位置，即速度场的不连续性。这就是给予偏移校正深度剖面的正常解释，而另一方面，它构成了地震图象的直观概念。

对一般非均匀的参考速度 $c_o(\underline{x})$，加权函数 W 必须用射线追踪法来确定。但，当 c_o 是常数且震源——检

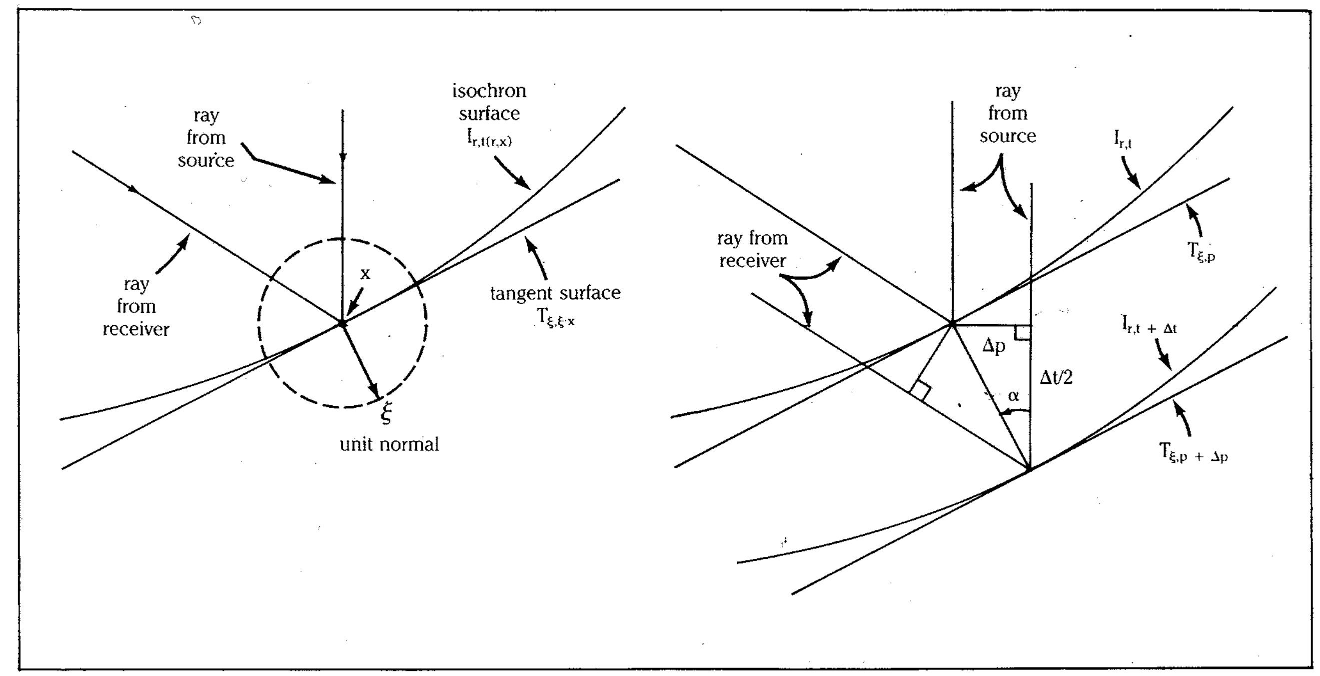

图 10.1–1 采用鉴别每一图象点相邻的等时面及其切面并随之在雷佟反演公式中做相应的改换变量的办法可得到地震的反演公式。

a) 固定一个图象点 $\underline{s}$ 和一个检波器 $\underline{r}$ 并假设 $c_o(\underline{x}) = 1$。设 $\underline{\xi}$ 为单位矢量，它等分震源射线和检波器射线之夹角。其次单位矢量 $\underline{\xi}$ 在切点 $\underline{x}$ 垂直于等时面 $I_{\underline{r},t(\underline{r},\underline{x})}$ 及其切面 $T_{\underline{\xi},\underline{x}\cdot\underline{\xi}}$。

b) 一级近似

$t(\underline{r},\underline{x}+\Delta\underline{x}) \approx t(\underline{r},\underline{x}) + (\nabla_x t(\underline{r},\underline{x}))\cdot\underline{x}$

导出以下等式：

$I_{\underline{r},t(\underline{r},\underline{x})+\Delta t} \approx T_{\underline{\xi},\underline{x}\cdot\underline{\xi}+\Delta t/2\cos\alpha}$

式中 α 是 $\underline{\xi}$ 和震源射线之间的夹角。根据该公式及雷佟变换的性质，在改变注标即 $f^{\hat{}}(\underline{\xi},p/a) = |a|\, f^{\hat{}}(a\underline{\xi},p)$ 情况下，有下列形式，

$$\frac{\partial^2}{\partial p^2} f^{\hat{}}(\underline{\xi},\underline{\xi}\cdot\underline{x}) \approx 8\cos^3\alpha\, \frac{\partial^2}{\partial p^2} f^{+}(\underline{r},t(\underline{r},\underline{x}))$$

代入式 7 并在雷佟公式 8 中改换变量 $(\underline{\xi},p)$ 改为 $(\underline{r},t)$，我们得到式 9 和 10。

Fig. 10.1–1 The seismic inversion formula can be obtained by identifying isochron surfaces in the neighborhood of each image point with their respective tangent planes and then making a corresponding change of variables in the Radon inversion formula.

a) Fix an image point $\underline{s}$ and a receiver $\underline{r}$ and assume $c_o(\underline{x}) = 1$. Let $\underline{\xi}$ be the unit vector bisecting the source and receiver rays. Then $\underline{\xi}$ is the unit vector normal to the isochron surface $I_{\underline{r},t(\underline{r},\underline{x})}$ and its tangent plane $T_{\underline{\xi},\underline{x}\cdot\underline{\xi}}$ at their point of tangency $\underline{x}$.

b) The first-order approximation

$t(\underline{r},\underline{x}+\Delta\underline{x}) \approx t(\underline{r},\underline{x}) + (\nabla_x t(\underline{r},\underline{x}))\cdot\underline{x}$

leads to the identification

$I_{\underline{r},t(\underline{r},\underline{x})+\Delta t} \approx T_{\underline{\xi},\underline{x}\cdot\underline{\xi}+\Delta t/2\cos\alpha}$

where α is the angle between $\underline{\xi}$ and the source ray. From this identification and the properties of the Radon Transform under a change of scale — viz, $f^{\hat{}}(\underline{\xi},p/a) = |a|\, f^{\hat{}}(a\underline{\xi},p)$ — it follows that

$$\frac{\partial^2}{\partial p^2} f^{\hat{}}(\underline{\xi},\underline{\xi}\cdot\underline{x}) \approx 8\cos^3\alpha\, \frac{\partial^2}{\partial p^2} f^{+}(\underline{r},t(\underline{r},\underline{x}))$$

Substituting from Eq. 7 and changing variables from $(\underline{\xi},p)$ to $(\underline{r},t)$ in the Randon formula, Eq. 8, we obtain Eq. 9 and 10.

波器距离一定时，W 可用解析法确定。例如，用零偏置面做试验，即 $\underline{s} = \underline{r} = (r_1, r_2, r_3 = 0)$，并且背景速度为常数，方程 9 变为

$$<f(\underline{x})> = \frac{16}{C_o^3}\int_{r_3=0} d^2\underline{r}\,\frac{x_3}{|\underline{x}-\underline{r}|}u_{sc}(\underline{r}, t = 2|\underline{x}-\underline{r}|/c_o) \quad \cdots\cdots \quad (11)$$

该式与吉尔荷夫偏移校正的经典公式相类似。(Sichneider, 1978; 还可参考 Norton 和 Linzer, 1981)。

模拟试验

图 10.1-2 和 3 示出一个上述偏移校正算法的模型，专用于二维偏移校正。该模型由一个固定震源和若干点状散射体组成，这些散射体之间的距离大致为震源主频率一个波长的长度，其分布呈 S 形。检波器安置在地面和位于散射体两侧的两个井内。图 10.1-3 的图象说明用不同的数据子集得到的分辨率。按照图 10.1-2 中所有检波器的排列位置做一个模拟零偏置试验，图10.1-4示出了根据此试验重新构成的 S 形和均匀的方块图象。

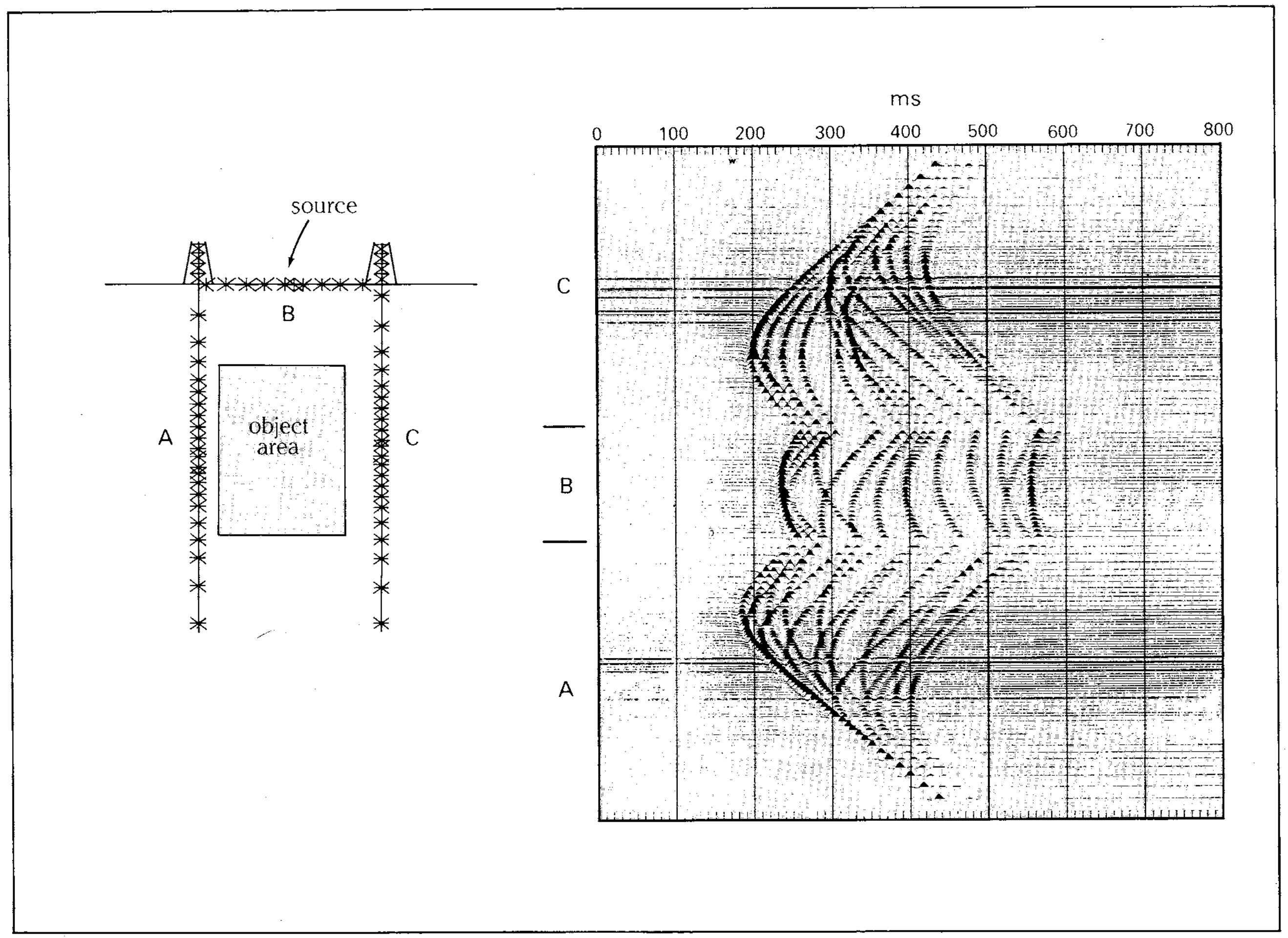

图 10.1-2 如图示尺寸的单震源、多检波器声波试验的模拟数据图。这些数据是运用类拟方程 6 的二维方程计算出来的。

Fig. 10.1-2 Synthetic data from a single-source, multiple-receiver acoustic experiment with the geometry as shown. The data was computed using the 2-D analog of Eq. 6.

$$<f(\underline{x})> = \frac{16}{C_o^3}\int_{r_3=0} d^2\underline{r}\,\frac{x_3}{|\underline{x}-\underline{r}|}u_{sc}(\underline{r}, t = 2|\underline{x}-\underline{r}|/c_o) \quad \cdots\cdots \quad (11)$$

which resembles the classical formula for Kirchhoff migration (Schneider, 1978; Norton and Linzer, 1981).

Synthetic Examples

Figures 10.1-2 and -3 show a synthetic example of the migration algorithm described above, specialized to a two-dimensional geometry. The model consists of a fixed source and point scatterers, which are separated by roughly one wavelength at the central frequency of the source and distributed to form the letter S.

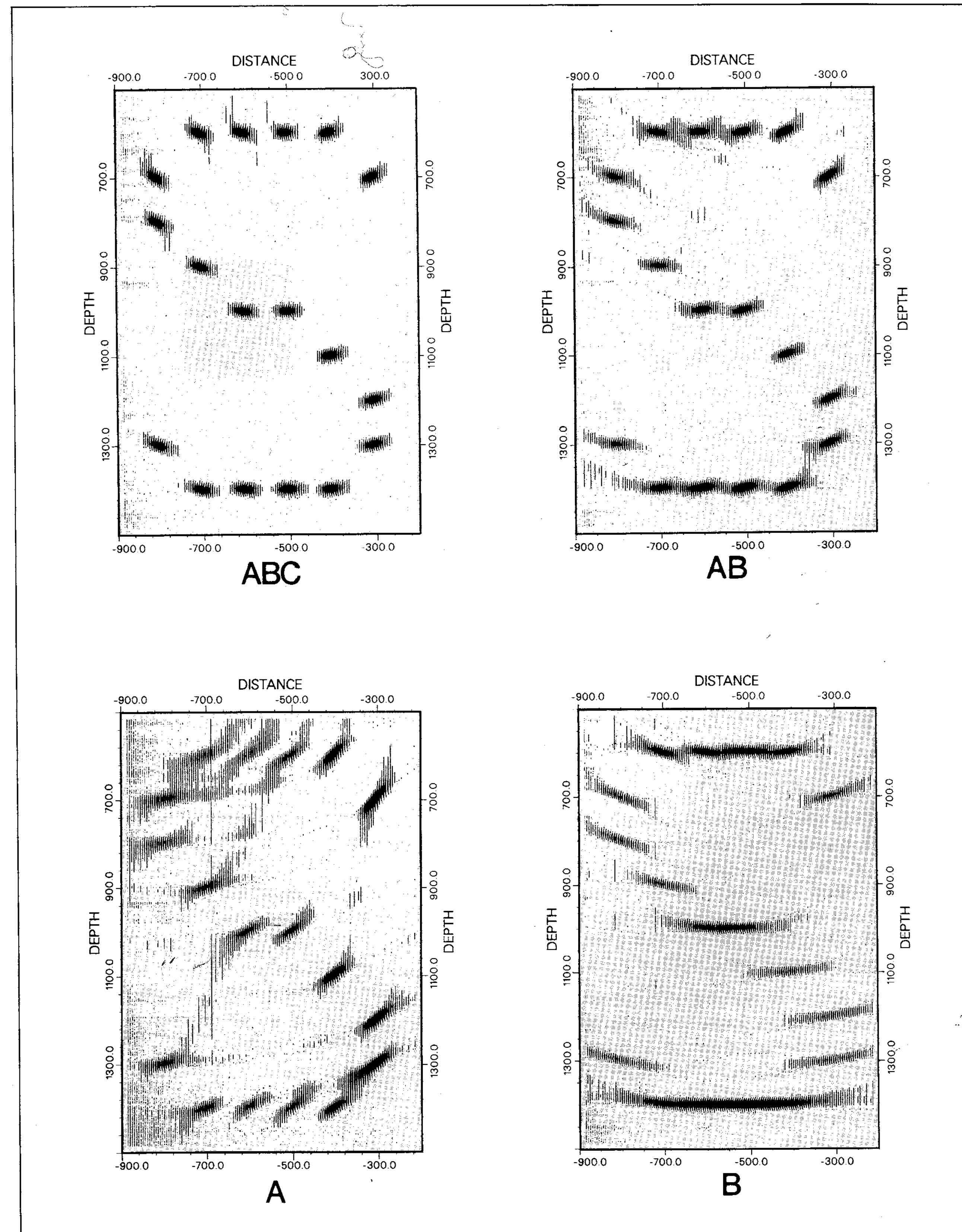

图 10.1-3 对图 10.1-2 (ABC) 的全部数据左边井十地面(AB)相应的数据子集、仅左边井(A)相应的数据子集和仅地面(B)相应的数据子集运用类似 9 式的二维方程所得出的点状散射体图象。

Fig. 10.1-3 Images of point scatterers obtained by applying the 2-D analog of Eq. 9 to all the data (ABC) of Fig. 10.1-2 and to the subsets of the data corresponding to the left borehole + surface (AB), left borehole only (A), and surface only (B).

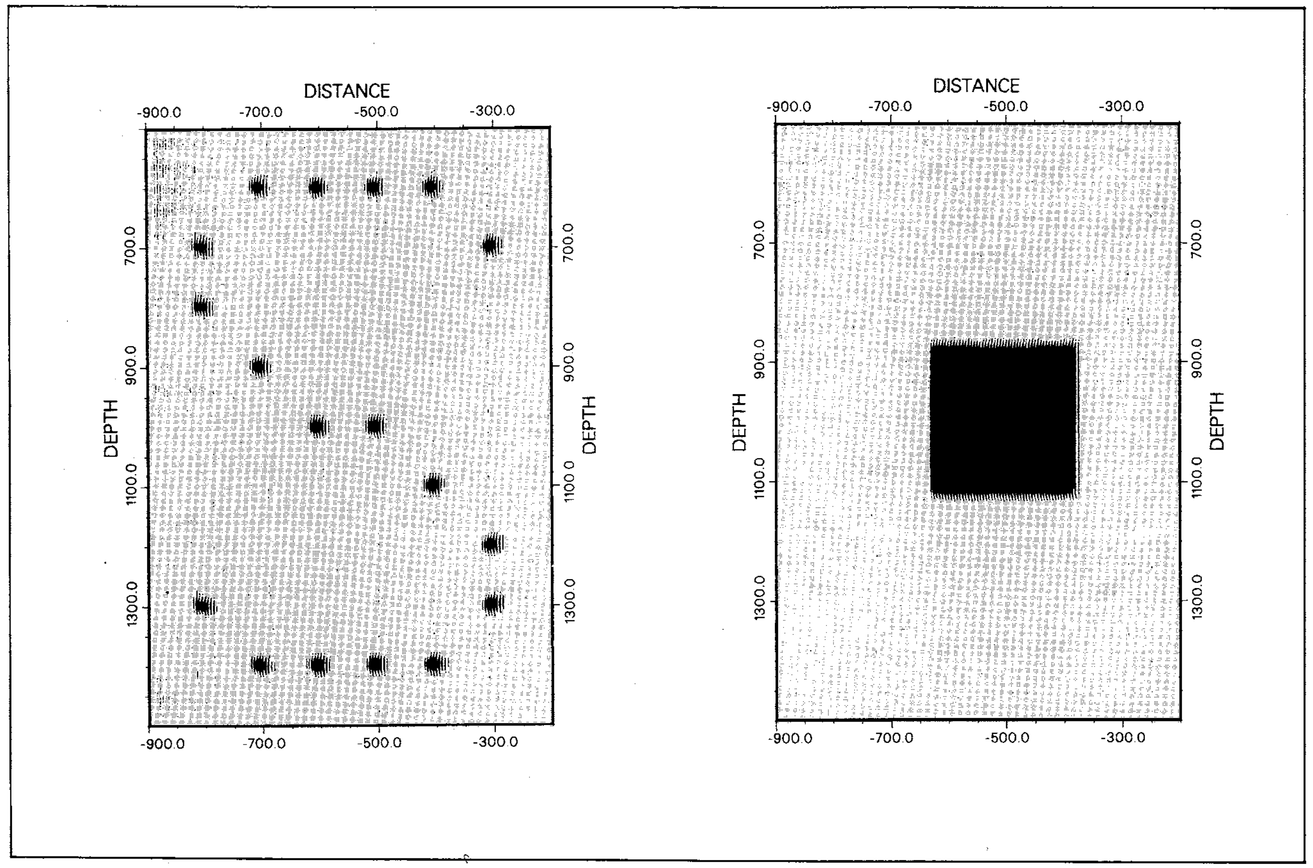

图 10.1-4 对在图 10.1-2 的设置中，由一组点状散射体和一个均匀方块组成的目的区表示震源 / 检波器试验的模拟数据运用类似11式的二维方程得出的图象。

Fig. 10.1-4 Images obtained by applying the 2-D analog of Eq. 11 to synthetic data representing coincidental source/receiver experiments in the geometry of Fig. 10.1-2 for objects consisting of a family of point scatterers and of a homogeneous square block.

Receivers were located both on the earth's surface and in two wells flanking the scatterers (Fig. 10.1-2). The images in Fig. 10.1-3 illustrat e the resolution obtained by using different subsets of the data. Fig. 10.1-4 shows reconstructions of the letter *S* and a homogeneous block, based on a synthetic zero-offset experiment using all the receiver positions in Fig. 10.1-2.

The images in figures 10.1-3 and -4 begin to answer some of the questions that a rise in dealing with both surface and borehole seismic data: e.g., What difference does it make to perform just surface experiments, or just VSP, or both? What would be the configuration of an ideal experiment (though we might not be able to perform it)? How do the initial assumptions about the structure affect the image?

All of these questions can be formulated as one; namely, What is the spatial resolution of a seismic experiment and migration (or inversion) algorithm and how does it depend on the geometry of the experiment, the reconstruction algorithm, and our assumptions about the medium? Providing answers to these questions is one of the most promising areas of research in seismic data processing.

References

1. Beylkin, G.: *Generalized Radon Transform and its Applications*, Ph.D., Thesis, New York University, New York (1982).
2. Deans, S.R.: *The Radon Transform and some of its Applications*, J. Wiley & Sons, New York (1983).
3. French, W.S.: "Computer Migration of Oblique Seismic Reflection Profiles," *Geophysics* (1975), vol. 40, p. 961–980.
4. Gazdag, J. and Sguazzero, P.: "Migration of Seismic Data," *Proc.*, IEEE (1984), vol. 72, p. 1302–1315.
5. Hagedoorn, J.G.: "A Process of Seismic Reflection Interpretation," *Geophysical Prospecting* (1975), vol. 2, p. 85–127.
6. Miller, D., Oristaglio, M., and Beylkin, G.: "A New Formalism and an Old Heuristic for Seismic Migration," Extended Abstract, 54th Annual Mtg. SEG, Atlanta (1984).
7. Norton, S.J. and Linzer, M.: "Ultrasonic Reflectivity Imaging in Three Dimensions: Exact Inverse Scattering Solutions for Plane, Cylindrical, and Spherical Apertures," IEEE *Trans. Biomed. Eng.* (1981), BME-28, p. 202–220.

图 10.1-3 和4 中的图象开始回答在处理地面和井下地震数据时产生的若干问题，如只作地面试验或只做 VSP 试验，或者两者都做，有什么差异？理想的试验应该是什么样的（尽管我们也许做不出来）？有关结构的初步设想怎样影响图象？

所有这些问题可归结为：即地震试验和偏移校正（或反演）算法的空间分辨率是什么？它如何取决于试验的几何尺寸、所采用的算法和我们对介质的假设？给出以上问题的答案是地震数据处理研究领域中最有意义的课题之一。

8. Robinson, E.A.: *Migration of Geophysical Data*, International Human Resources Development Corporation, New York (1983).
9. Schneider, W.: "Integral Formulation for Migration in Two and Three Dimensions," *Geophysics* (1978), vol. 43, p. 49–76.